



Role of carbon clusters in high-order harmonic generation in graphite plasmas

RASHID A. GANEEV,^{1,3}  GANJABOY S. BOLTAEV,¹  KE ZHANG,¹ SANDEEP KUMAR MAURYA,¹ MOTTAMCHETTY VENKATESH,¹ ZHI YU,¹ VYACHESLAV V. KIM,¹ PAVEL V. REDKIN,¹ AND CHUNLEI GUO^{1,2,4}

¹The Guo China-US Photonics Laboratory, State Key Laboratory of Applied Optics, Changchun Institute of Optics, Fine Mechanics and Physics, Chinese Academy of Sciences, Changchun 130033, China

²The Institute of Optics, University of Rochester, Rochester, NY 14627, USA

³rashid_ganeev@mail.ru

⁴guo@optics.rochester.edu

Abstract: Laser ablation is able to produce plasmas containing neutrals, ions, clusters, and nanoparticles, which can all act as emitters of harmonics from ultrashort laser pulses. Here the efficient low- and high-order harmonic generation (HHG) of femtosecond pulses from the carbon plasmas produced by nanosecond pulses is demonstrated. The efficiencies of harmonic generation from carbon clusters are analyzed using delayed ablation of graphite. We show that carbon clusters can be considered as the sources of efficient harmonics in the 40-100 nm spectral range. This approach of harmonic generation from the plasmas in double-pulse configuration of HHG can be applied for studying other clusters to determine the best conditions for HHG and the influence of multi-particle species on the nonlinear optical processes.

© 2019 Optical Society of America under the terms of the [OSA Open Access Publishing Agreement](#)

1. Introduction

High-order harmonic generation (HHG) in isotropic media can provide table-top sources in generating coherent extreme ultraviolet (XUV) radiation [1]. Therefore, it is important to analyze high-order nonlinear optical properties of materials through the search for enhancement of harmonic yield from different isotropic media (gases [2], and plasmas [3]). Particularly, the conditions for efficient emission of coherent XUV radiation through HHG in different clusters using ultrashort laser pulses should be studied, which have further application in a range of fields from physics, to chemistry and to biology.

HHG conversion efficiency in XUV range is limited due to a range of factors that prevent the generation of sufficient fluencies of coherent short-wavelength radiation. The best results (10^{-5} in the case of gas and plasma HHG and 10^{-4} for resonantly enhanced single harmonic of 800 nm radiation) show some limitations of harmonic generation efficiency. The phase mismatch, low density of media and limitation in laser intensity further restrict harmonic generation efficiency in isotropic medium [4]. Currently, significant research efforts are shifted towards attosecond pulse generation in the case of gas media [5], nonlinear spectroscopy of plasmas through single harmonic generation in the case of plasmas [6], quasi-phase matching (in the cases of gases [7] and plasmas [8]) and HHG studies using clusters, quantum dots and nanoparticles in the cases of plasmas [9] and gases [10].

Another emerging field is HHG in solid bulk media, for example in ZnO or ZnSe [11]. In that case, different channels including intraband and interband processes were considered for explanation of the harmonic generation using mid-infrared driving pulses. HHG in solids could also become relevant for nanoparticles. From this perspective, clusters, quantum dots and large nanoparticles may act as an intermediate material between atoms and solids.

The studies of HHG using clusters, quantum dots and nanoparticles require analysis of the plasmas, which contain multi-particle species, to temporally match them with the propagation of driving femtosecond pulses through the plasmas. In the past, the plasma formation for HHG was achieved with a picosecond laser pulse heating [6,8,9], and the optical delays between the heating picosecond pulses and driving femtosecond pulses originated from the same laser were usually less than 100 ns. Meanwhile, to match the propagation of the driving pulses and the highest concentration of the studied groups of multi-particle species and to confirm or disapprove the assumption of the variation of the velocities of different components, one has to find other methods to form the optimal delay between the heating and the driving pulses to maximize HHG efficiency.

The earlier reported studies of HHG from gases and during ablation of cluster and nanoparticle targets have revealed the advantages of using such species for frequency conversion in XUV range. Larger cross-section of recombination, possibility of recombination of accelerated electron with parent multi-particle through either recombination with the same atom or neighboring atom, or the multi-particle as a whole were considered as the most probable reasons in enhancing HHG yields from such clustered plasmas. However, there has been no study in optimizing the delay between heating and driving pulses in the microsecond timescale assuming the hypothesis of the slower velocities for larger-sized species. Notice that, even without this optimization, the harmonic yields from ablated multi-particle targets higher than from ablation of bulk targets of the same material leading to the formation of single atomic/ionic plasmas. Here the meaning of multi-particle target refers to the one containing the clusters, quantum dots or nanoparticles glued on the surface of different substrates.

The most probable reason for harmonic enhancement was attributed to the appearance of small clusters in the area of femtosecond pulse propagation at relatively small optical delays. Their appearance in that area was assumed once estimating their velocities and delays between the beginning of ablation and propagation of femtosecond pulse at the fixed distance above the target surface. Particularly, for most of HHG experiments, these distances were maintained at ~ 0.2 mm, while the delay for each target was chosen to be 20 to 80 ns depending on the atomic weight of the elements comprising different targets. Particularly, the maximal harmonic yield from ablated graphite has earlier been achieved at ~ 30 ns, which allows calculating the velocity of atoms and ions spreading out from the target ($\sim 6 \times 10^3$ m s $^{-1}$). At the same time, ablation of the fullerenes comprising 60 atoms of carbon led to similar “optimal delay” at which maximal yield of harmonics was achieved. Correspondingly, one could assume the similarity in the velocities of carbon single atoms and C₆₀ at the conditions of ablation using picosecond heating pulses. Similar feature has also been observed in the case of carbon nanotubes.

Another important concept allowing the enhancement of harmonic yield is the application of the two-color pump (TCP) of generating medium, when two fields simultaneously participate in the HHG process. This concept has earlier been demonstrated in the case of gases and ablated bulk materials. Earlier studies of HHG in gases have anticipated that stronger harmonics generation in the case of TCP was possible due to the formation of a quasi-linear field, selection of the short quantum path component, which has a denser electron wave packet, and higher ionization rate compared with single-color pump (SCP) [12]. The orthogonally polarized second field can also be responsible in the modification of the trajectory of accelerated electron from being two-dimensional to three-dimensional that may lead to removal of the medium symmetry. With suitable control of the relative phase between the fundamental and second harmonic radiation, the latter field enhances the short path contribution, resulting in a clean spectrum of harmonics. One can expect that TCP of clusters can further enhance the harmonic yield even at small ratios of second and first waves' intensities provided the sufficient overlap of these two fields in the medium under consideration.

In this work, we introduce, for the first time, a new scheme of nanosecond pulse heating and femtosecond laser pulse driving for HHG. The synchronization of two laser sources, such as most commonly used Ti: sapphire and Nd:YAG lasers, may resolve, to some extent, the puzzle related to the enhancement of harmonics in the multi-atomic species produced during ablation of the bulk materials or the targets initially contained multi-atomic components. The main advantage of this approach is that we can control the delay between the heating nanosecond pulses and the driving femtosecond pulses over a wide range between 0 and 10^5 ns, which assumes to be sufficient for analysis of the fast and slow components spreading in the laser-produced plasmas. The use of nanosecond Nd:YAG lasers as the sources of heating pulse may also offer some additional advantages compared with the commonly used picosecond pulses of the same pulse repetition rate and wavelength as the driving sources. The application of nanosecond pulses to ablate the surface of targets under consideration may allow the formation of less ionized and excited plasma during longer period of laser-matter interaction compared with picosecond pulses. This conclusion is based on the analysis of the nanosecond and picosecond ablation induced plasma emission in the visible and XUV ranges in the case of formation of the “optimal” plasmas leading to generation of highest harmonic yields. Notice that such plasmas formed by picosecond pulses have demonstrated stronger incoherent XUV emission. Additionally, Nd:YAG lasers commonly operating at 10 Hz pulse repetition rate are more suitable for stable HHG in plasmas compared with 1-kHz picosecond pulse ablation, though in the latter case some tricks such as target rotation can partially mitigate the stability of 1-kHz coherent short-wavelength sources.

The first attempts in frequency conversion at such conditions were reported in the case of the studies of the lowest-order harmonic generation from the ablated carbon-containing materials [13]. Third harmonic (TH) in the laser plasmas produced on the surfaces of different materials was analyzed using the delays ranging between a few tens nanosecond to a few hundred microsecond between a 7-ns heating pulse and a 17-ns driving pulse, both of 1064 nm in wavelength. The observation of TH emission, though extremely weak, at the microsecond timescale of delays allowed concluding that the process of third harmonic generation (THG) occurs not only from atoms and ions of carbon materials at small delays but also from their aggregates at large delays.

This approach is extremely useful for the analysis of multi-atomic systems as the media for HHG. In this paper, we demonstrate, for the first time, the HHG in graphite plasma using a broad range of delays between a 5-ns heating pulse and a 40-fs driving pulse. We show the advantages of using nanosecond pulses for plasma formation to achieve the efficient HHG compared with picosecond pulses induced ablation. The TCP concept of laser-clusters interaction demonstrates the advantages in generation of odd and even harmonics. This study allows us determining the optimal delay between the heating and driving pulses for both monoparticles and multi-particle aggregates and to generate harmonics from those species. Our studies show that small carbon clusters arrive at the area of interaction with femtosecond beam notably earlier than one can expect assuming the kinetic consideration when the components are assumed to reach thermodynamic equilibrium during the expansion. Our observations allow concluding that all carbon clusters acquire from the very beginning a similar kinetic energy and spread out of surface with the velocity approximately similar to the one that possesses a single carbon atom ablating from the bulk material.

2. Experimental

Two groups of experiments were carried out to analyze the role of carbon clusters in harmonic generation by studying the influence of delay between heating and driving pulses on the frequency conversion of the latter pulses. In the first set of studies we analyzed TH yield from graphite plasma, and in the second group of experiments we generated high-order harmonics and measured their yield by varying the delay, fluence of heating pulse, driving pulse energy, SCP and TCP of laser-produced plasma.

In the case of THG studies the laser radiation ($\lambda=800$ nm, $\tau=40$ fs, 1 kHz; Spitfire Ace, Spectra-Physics) was focused by a 400 mm focal length lens at a distance of 0.6 mm above the targets surface on the plasma produced by ablation in vacuum chamber of bulk graphite using picosecond (1 kHz, 800 nm, 0.5 mJ, 200 ps) or nanosecond (10 Hz, 1064 nm, 5 mJ, 5 ns, Q-Smart, Coherent) pulses (Fig. 1). The beam waist diameter of the focused femtosecond radiation was $76\text{ }\mu\text{m}$. The spectral characteristics of TH radiation ($\lambda=266$ nm) were analyzed by a spectrometer (USB2000, Ocean Optics). To create plasma plume using picosecond pulses, a pulse was split from the Ti: sapphire laser by a beamsplitter before the compression of fundamental uncompressed pulse. This radiation was focused on the target to heat it and to produce plasma either in the vacuum or air conditions. The diameter of ablation zone was adjusted to be approximately 0.25 mm. An optical delay between heating (picosecond) and driving (femtosecond) pulses was varied between 5 and 60 ns, while an electronic delay between nanosecond and femtosecond pulses allowed to apply sufficiently longer delays between the two pulses (i.e. up to 10^5 ns).

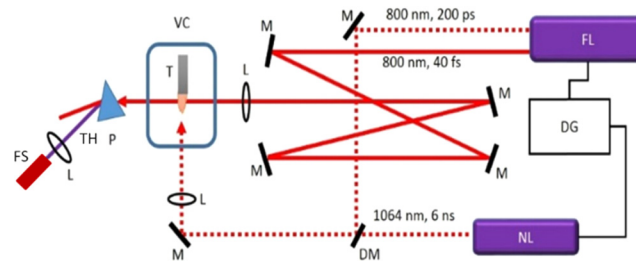


Fig. 1. Third harmonic generation arrangement. FL, femtosecond laser; NL, nanosecond laser; DG, digital generator; M, mirrors; DM, dichroic mirror; L, lenses; VC, vacuum chamber; T, target; P, prism; TH, third harmonic emission; FS, fiber spectrometer.

The graphite plasma was also used for HHG (Fig. 2). The femtosecond pulse propagated through the plasma 30 ns from the beginning of target irradiation by 200 ps or 5 ns heating pulses. This delay between heating and pump pulses was proven to be optimal for HHG in graphite plasma at the used geometry of experiments when the 800 nm driving femtosecond pulses were focused onto the plasma from the orthogonal direction, at a distance of 0.2 mm above the target surface, contrary to the TH studies when this distance was maintained at 0.6 mm.

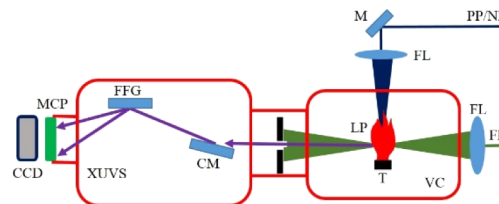


Fig. 2. Setup for high-order harmonic generation. PP, converting femtosecond pulses, PP/NP, picosecond or nanosecond heating pulses; FL, focusing lenses; VC, vacuum chamber; T, target; LP, laser plasma; XUVS, extreme ultraviolet spectrometer; CM, cylindrical gold-coated mirror; FFG, flat field grating; MCP, microchannel plate; CCD, CCD camera.

The harmonic yield was maximized by adjusting the position of the target with regard to the optical axis of propagation of the driving femtosecond pulses and by varying the focusing position relative to the plasma. The harmonic emission was directed to the XUV spectrometer, which contained a cylindrical mirror and a 1200 grooves/mm flat field grating with variable

line spacing. The XUV spectrum was recorded by a micro-channel plate (MCP) with phosphor screen, which was imaged by a CCD camera.

Some of the experiments were carried out using two-color pump (TCP) of graphite plasma. The reason for using TCP instead of single-color pump (SCP) was related with earlier demonstrated advantages of this approach in generating the odd and even harmonics, as well as larger efficiency of harmonic yield. TCP using the 800 nm radiation as the first field and 400 nm radiation as the second field were applied to carry out the comparative analysis of TCP and SCP schemes. The 0.4-mm-thick barium borate crystal (BBO, type I) was installed inside the vacuum chamber on the path of focused the 800 nm pulse. The conversion efficiency of H₂ pulses ($\lambda=400$ nm) was ~5%. The overlap of these two pulses in plasma area was sufficient for observation of the role of the second orthogonally polarized field influencing the whole process of HHG due to small group velocity dispersion in the thin BBO crystal.

Ablation of graphite in most of these HHG experiments was carried out using nanosecond pulses from Nd:YAG laser as well. Similarly to TH studies, two lasers were synchronized with each other. We analyzed the harmonic yield using electronically variable delay between the heating and driving pulses.

3. Third harmonic generation

The motivation for THG prior to HHG in clustered medium is related with two factors. Firstly, the analysis of different plasma species using this lower-order nonlinear optical process is less complex compared with HHG-based approach from the point of view of determining most suitable and efficient media, as well as most efficient conditions for harmonic generation. Secondly, the coincidence of the optimal delays between heating and driving pulses in the cases of lowest harmonic generation and HHG can provide additional information to determine the relation between the velocities of singly-atomic and multi-atomic species in plasmas.

Prior to the study of the frequency conversion in the graphite plasma, THG in air with variable driving pulse energy was performed which showed the anticipated cubic dependence of harmonic yield on the laser energy. THG in air was carried out in order to calibrate experimental setup and estimate TH conversion efficiency from carbon-containing plasma with regard to similar process in air.

Two sets of experiments were performed for THG study in the graphite plasma produced in vacuum. In the first case, the 200 ps pulses were used as a heating radiation to create C plasma. In the second case, 5 ns heating pulses were used for target ablation. The objective was to optimize the target position, the heating pulse energy, the delay between pulses, and the driving beam focal position to achieve the maximum TH yield from C plasma. These studies revealed the preference in application of nanosecond pulses for plasma formation to achieve higher conversion efficiency compared with picosecond heating pulses.

Figure 3(a) shows, how TH yield from C plasma increases with the growth of the driving pulse energy. Variation of TH intensity showed approximately cubic dependence by increasing the driving 40 fs pulse energy up to 500 μ J. An increase in the free-electron density was likely the limiting factor for the harmonic yield in early experiments with laser plasmas [14]. So the search for formation of “optimal” plasma from the point of view of larger conversion efficiency towards the shorter wavelength region is required, thus prompting us to analyze TH efficiency variations at different energies of heating nanosecond pulses. In present experiments the TH intensity was gradually increased with the growth of heating 5 ns pulses up to 3 mJ [Fig. 3(b)].

Harmonic intensity considerably depended on the distance between the optical axis of driving beam and graphite surface due to the variations of plasma concentration above the target at a fixed delay. Figure 3(c) shows the variation of TH intensity as a function of the distance between the target and the optical axis of the femtosecond pulse. TH from plasma was observed up to the distance of ~4 mm away from graphite target. It has been demonstrated earlier that the

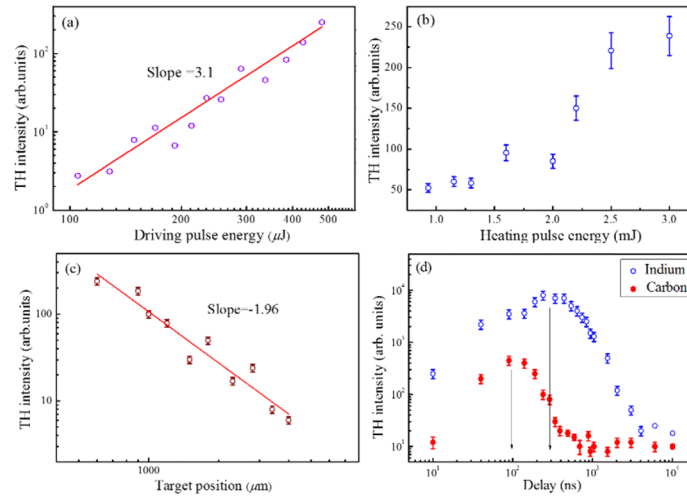


Fig. 3. (a) TH intensity as a function of driving pulse energy. No saturation of cubic $I_{\text{TH}}(E_{\text{DP}})$ dependence was observed along the whole range of variations of the driving pulse energy. (b) Influence of nanosecond heating pulse energy on the TH yield. (c) TH intensity as a function of the distance between graphite target and axis of femtosecond beam. The measurements were carried out up to 4 mm from the target surface. (d) Dependence of TH yield from graphite plasma on the delay between heating nanosecond pulse and driving femtosecond pulse (filled circles). Similar dependence is also shown in the case of indium plasma (empty circles). Arrows show the delays at which maximal TH yields were observed. The driving beam was focused at the distance of 0.6 mm above the target in all of these experiments excepting of these shown in (c). The delay between the heating and driving pulses was maintained at 100 ns during these experiments except of (d).

distribution of spreading species during ablation is controlled by their longitudinal velocity and strongly depends on input fluence [15]. The distribution of different species during ablation has direct influence on the TH intensity that resulted in the maximal harmonic yield close to the target surface. The variation of TH intensity at different distances between the optical axis of the driving beam and the target surface (x) was approximately close to reciprocal quadratic dependence [$I_{\text{TH}} \propto x^{-n}$, $n = 1.96$] at the nanosecond pulse fluence of 4 J cm^{-2} . Notice that parameter n can be varied by changing conditions of experiments, in particular the fluence of heating pulses. The delay between the heating and driving pulses was maintained at 100 ns during the THG experiments presented in Fig. 3(a-c), which was optimal assuming the 0.6 mm distance between the target and the optical axis of the femtosecond beam.

Early studies of laser ablation of graphite have revealed the typical characteristics of the expanding plasma species (average velocity $1.5 \times 10^3 \text{ m s}^{-1}$) for ablation with 532 nm, 10 ns pulses at fluencies of the order of 3 J cm^{-2} [16]. The measured mass distribution presented in [16] revealed the presence of C_5 to C_{25} species. Those carbon clusters, as has also been shown in other studies, have the largest population in the graphite plasma among other clusters. Earlier it was assumed that they may be a reason of such attractive feature as the more efficient harmonics generation with regard to similar process in single atomic/ionic media. In the meantime, large nanoparticles do not participate in the process of HHG, but rather may serve as the sources of the formation of smaller clusters during different stages of laser ablation due to partial disintegration of large multi-particle species during heating, melting, and evaporation. These stages of laser-matter interaction may cause formation of the notably smaller clusters containing a few tens of carbon atoms. Meanwhile, the remaining parts of large nanoparticles do not

participate in harmonic generation, but rather deposit later on the nearby surfaces. Thus the performance of nanomaterials for the applications in harmonic generation depends on their distribution and size at the moment of propagation of the femtosecond pulses through the plasma plume. Hence the precise control over dynamics of their appearance in the plasma is essential.

The temporal evolution of TH yield from C plasma was analyzed by varying the delay between the nanosecond pulses inducing ablation and the driving laser pulses [Fig. 3(d), filled circles]. The distance between target and femtosecond beam propagation in these TH experiments was maintained at ~ 0.6 mm. The maximal TH yield was observed at ~ 100 ns from the beginning of ablation. To prove the concept that this optimization depends on the mass of the particles participating in harmonic generation we used a heavier target (indium) ablated at similar fluence of heating pulses and other similar experimental conditions. A similar kinetic energy $E = mv^2/2$ can characterize the arrival of plasma components from different materials ablated at identical conditions. Correspondingly, one can expect the arrival of indium ions and atoms in the area of interaction with driving beam at $(M_{\text{In}}:M_{\text{C}})^{0.5} \sim 3$ times longer delay with regard to carbon particles taking into account the ratio between atomic weights of these two targets ($M_{\text{In}}:M_{\text{C}} \approx 9$).

This anticipated maximal yield of TH from indium plasma was observed in our experiments when we achieved highest TH efficiency at ~ 300 ns from the beginning of ablation of the indium target [Fig. 3(d), empty circles]. Thus, one can assume that this rule works properly for the dynamics of material spreading once one analyzes the particles movement during laser ablation at relatively moderate fluencies ($2\text{--}10 \text{ J cm}^{-2}$) of heating nanosecond pulses.

4. High-order harmonic generation

XUV emission spectra of carbon plasma at different regimes of graphite ablation in the range of 30–130 nm are shown in Figs. 4(a) and 4(b). We used either picosecond (upper panel) or nanosecond (middle panel) pulses for laser ablation (Fig. 2). Various emission lines attributed to CII – CIII ions were identified and used for calibration of our XUV spectrometer. These conditions of ablation were unsuitable for efficient HHG due to presence of large amount of free electrons preventing optimal phase relations between the driving and harmonic waves. We chose nanosecond pulses induced ablation for further analysis of HHG from different species of graphite plasma since in that case, contrary to ablation by picosecond pulses, we were able to analyze the delay-dependent harmonic emission at the delays between heating and converting pulses ranging between 0 and 5×10^4 ns.

Lesser excitation of graphite target by nanosecond pulses allowed formation of plasma suitable for harmonic generation [Fig. 4(c)]. Odd harmonics of 800 nm radiation up to 23rd order (H23) were observed. It is worth noting that our observations of harmonic spectra did not show a simultaneous presence of plasma emission from high-charged particles in the studied spectral range (30–130 nm) that confirms that these experiments were carried out at a soft ablation regime of carbon-containing target. The absence of the plasma emission associated with the higher-charged ions at these conditions was accomplished by the moderate excitation of graphite. The driving pulse at $I \approx 2 \times 10^{14} \text{ W cm}^{-2}$ also did not cause the appearance of strong ionic emission from the higher-charged carbon ions.

The important peculiarity of these plasma emission and harmonic studies was the proximity of some ionic transitions of carbon with the wavelengths of harmonics, particularly strong CII transitions (53.8 and 59.5 nm) and 15th and 13th harmonics (53.3 and 61.5 nm) respectively. Neither enhancement nor suppression of these harmonics generated in graphite plasma was observed. These studies showed that the proximity of strong emission lines and harmonics did not necessarily lead to variation of the harmonic yield.

The reason in presenting the experimental data as the images appearing on the screen of computer rather than the line-outs of HHG spectra is justified by better viewing of obtained data and clear definition of the difference between the plasma and harmonic spectra. The goal of

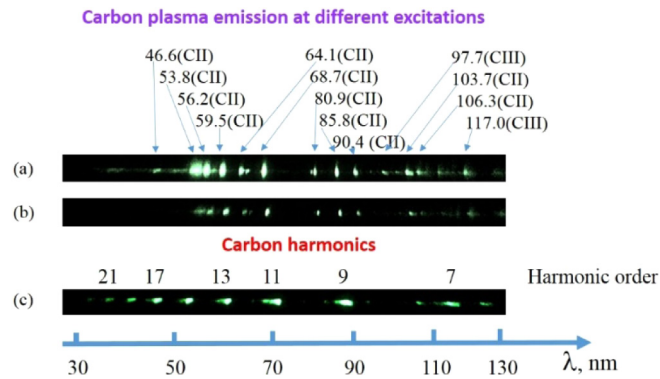


Fig. 4. Raw images of plasma and harmonic spectra. (a) Graphite plasma emission using picosecond pulses induced ablation. (b) Graphite plasma emission using nanosecond pulses induced ablation. (c) Harmonic spectra using single-color pump (800 nm) of C plasma at 30 ns delay between heating and driving pulses. The fluence of heating pulses on the target surface was maintained at 5 J cm^{-2} . The distance between the target and the axis of propagation of the driving beam was 0.2 mm.

this group of studies was the qualitative determination of the influence of different conditions of ablation on the plasma emission and the harmonics conversion efficiency rather than the quantitative measurements of harmonics in the plasmas. Also notice that visual analysis of the raw images of harmonics and plasma emission allows distinguishing these sources of XUV radiation by their divergences. The vertical dimensions of the raw images of plasma emission, which characterize its divergence, were a few times larger compared with those of harmonics. Additional advantage of this method of data presentation is a direct demonstration of the insignificant role of emission lines in the harmonic conversion efficiency. The approximately plateaulike shape of harmonics distribution remained unchanged in spite of coincidence of plasma emission lines and some harmonics orders.

The λ -axis in Fig. 4 is shown on the basis of the calibration of XUV spectrometer for distinguishing the distribution of harmonics along the short-wavelength region. The saturated images were intentionally chosen to present the spectra for better viewing. Note that the unsaturated images were used for the line-outs of the HHG spectra.

Next set of HHG studies was performed using two orthogonally polarized driving beams. The 0.4 mm thick BBO crystal was inserted on the path of 800 nm radiation inside the vacuum chamber that allowed generation of 400 nm pulses (H2), while maintaining sufficient temporal and spatial overlap of 800 and 400 nm pulses in C plasma. Even small conversion efficiency ($\sim 2\%$) of 400 nm radiation allowed generation of the lower-order even harmonics alongside with the odd ones (Fig. 5). We were able achieving the even harmonics generation up to H14 (see middle panel). Relatively small yield of lower-order harmonics in these spectra (H6 to H9) was caused by weaker sensitivity of MCP in the range of the wavelengths above 100 nm. The use of different fluencies of heating nanosecond pulses ranging between 5 and 9 J cm^{-2} led to variations of generated spectra.

The conversion efficiency of odd harmonics in the case of two-color pump was approximately three times higher than in the case of single-color pump. One can see that even at very small ratio of 400 and 800 nm pulse energies (1:20) the influence of weak field was sufficient to strongly modify the whole harmonic spectrum.

Application of two-color sources for HHG has also another advantage. It allows the two-fold increase of the number of generated harmonics, which in turn may lead to observation of the resonance-induced enhancement of single components of those multiharmonic sources. The

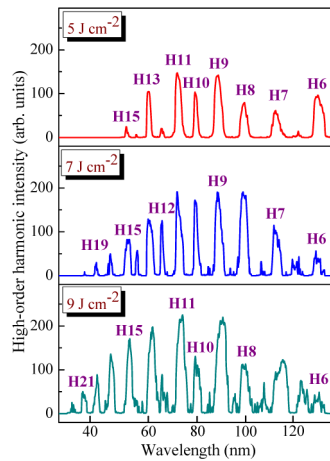


Fig. 5. Harmonic spectra using the two-color pump (800nm + 400 nm) at different fluencies of nanosecond pulses on the target surface. One can see some red shift of odd harmonics at highest fluence while even harmonics remained at fixed wavelengths.

latter process is mostly related with the ionic transitions of various materials possessing high oscillator strengths. In the case of graphite plasma, we did not see the enhancement of even harmonics, while in the case of indium plasma H12 was notably enhanced alongside with H13 due to proximity with the ionic transition possessing large oscillator strength [17].

In the case of stronger excitation of carbon plasma we observed the small red shift of odd harmonics, while even harmonics were not shifted due to notably weaker energy of 400 nm radiation compared with 800 nm pulses (bottom panel of Fig. 5). Previous reports on gas HHG experiments have shown a distinct difference between the HHG spectra driven by negatively and positively chirped pulses, which was related with both the influence of the dynamically induced negative chirp and the positive chirp induced by strong laser radiation and the ionized medium due to the self-phase modulation of the laser pulse [18]. The observation of red-shifted harmonics has been analyzed in [19] during gas HHG studies, while the blue-shifted harmonics is a common feature observed in multiple studies of HHG from the gases and plasmas. Notice that the red-shift of chirp-free pulses in the case of dense plasmas has already been reported in the case of plasma harmonics studies [20].

Different scenarios can be involved in the case of clustered media in regards to the observed redshift of odd harmonics with higher intensities of the nanosecond ablating pulse. It has been shown in [19] that the chirp-induced shifts of harmonics generated in a Xe gas jet exhibit a trend toward either the blue or red, depending on the particle density. The authors point out that redshift was observed at low gas densities. They suggest that this process might be related to the Kerr effect, electron-ion recombination, and ion expansion and cluster formation. The latter mechanism seemed consistent with our experimental findings. The chirp-induced redshift and blueshift were explained by the model including both atoms and ions. The neutrals were assumed to be responsible for the blue-shift, while the ions were the main reason for the redshift. The redshift can also be attributed to the self-phase modulation (SPM) of the laser pulse during the propagation of the leading part of the pulse through the medium consisting of neutrals and singly charged ions. As one can see, the broader spectra of odd harmonics (Fig. 5, bottom panel) from C clusters can also be attributed to the influence of SPM, leading to the redshift of those harmonics. Thus our observations of the redshifted odd harmonics were consistent with the model described in [19].

We did not measure the plasma density in these experiments. The heating radiation intensity on the target surface was maintained at $2 \times 10^9 \text{ W cm}^{-2}$. The particles density in plasma was estimated using the hydrodynamic code HYADES [21] to be a few units of 10^{17} cm^{-3} . The ionization potentials of carbon atoms and singly charged ions are equal to 11.25 and 24.38 eV, respectively. Thus such plasma mainly consists of excited neutral atoms and singly ionized carbon. Notice that the presence of excited atoms and ions can increase a nonlinear optical response of laser-produced plasma.

A typical dependence of the 9th and the 17th harmonics intensities on the delay between pulses is presented in Fig. 6. At initial stages of plasma formation and spreading out of the targets surface, i.e. at the delays less than 10 ns, the concentration of neutrals and singly charged ions is insufficient to produce a measurable amount of harmonic photons, since the whole ensemble of particles possessing the velocities of $\leq 1 \times 10^4 \text{ m s}^{-1}$ cannot reach the optical axis of the propagation of driving beam, which was $\sim 0.2 \text{ mm}$ above the graphite surface in present experiments. The increase of delay up to 10 to 50 ns caused the appearance of a large amount of carbon atoms and ions, as well as light clusters, along the path of femtosecond beam that allowed maximizing the yield of harmonics. The increase of delay above 50 ns led to a decrease of HHG efficiency. We observed a similarity in the delay dependence for H9 and H17. The harmonics almost disappeared from XUV spectra once the delay exceeded 300 ns. Our attempts to observe the harmonic emission in the microsecond time scale of delays were unsuccessful.

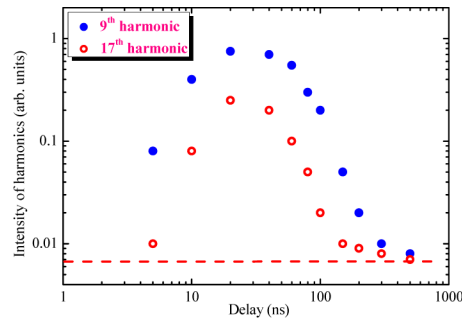


Fig. 6. Dependences of H9 and H17 yields on the delay between nanosecond and femtosecond pulses. Dashed line shows the threshold of registration of harmonic emission.

5. Discussion

Clusters play important role in modification of the harmonic spectra generating in different media. The harmonics' enhancement in the gas jets containing clusters has been reported in [10]. In the case of clusters the cross-section of recombination of the accelerated electron with the parent particle is higher compared with the atoms [22]. In the meantime, the experiments with gas clusters have revealed some difficulties in disentangling the harmonics produced by different species (monomers and clusters of different sizes). The uncertainty in the exact mechanism of the HHG from clusters has previously been underlined in [22,23].

Laser ablation of carbon has been proven to be a versatile method for the synthesis of clusters, which allowed characterization and dynamics of the multi-particle species formation [24]. The authors of [25] have concluded that the appearance of clusters during ablation is a result of clusters ejection from the target and collision-related aggregation in the expansion of the plume. The growth of clusters is based on the addition of many small carbon neutral species to the ions in a stepwise fashion. The processes that can cause formation and disintegration of multiatomic species include photomechanical ejection, liquid phase ejection and fragmentation, homogeneous nucleation and decomposition, heterogeneous decomposition, etc. [26].

A detailed understanding of the basic physical processes governing the composition of carbon ablation and the reliable methods for controlling the plume species became a necessity for selection of the optimal plasma conditions for HHG. The following arguments supporting the explanation of higher yield of harmonics from such plasmas were considered: (i) carbon species allow the formation of multi-particle clusters during laser ablation, which can enhance HHG yield, (ii) the first ionization potential of carbon is high enough to prevent the appearance of high concentration of free electrons, (iii) the graphite target allows easier generation of a relatively dense carbon plasma and the production of phase-matching conditions for lower-order harmonic generation. The carbon-containing materials like graphite, fullerenes, and carbon nanotubes have proven that, at optimal ablation conditions, they can be considered as attractive plasma media for efficient harmonic generation in the 40–80 nm spectral range using the femtosecond laser pulses [27].

To define the role of clusters in variation of nonlinear optical response of medium during frequency conversion of ultrashort pulses one has to analyze both lowest- and higher-order harmonic generation conditions. As already mentioned, the necessity in lowest-order harmonic generation studies is as follows. It provides a guide for selection of the targets suitable for the efficient generation of short-wavelength coherent radiation using different delays between heating and driving pulses [28]. This method also allows the application of low-order harmonic generation for plasma diagnostics, which is less complex compared with HHG-based method. Additional assumption for strong harmonics generation from clusters and nanoparticles compared with single atoms or ions could be the higher concentration of neutral atoms inevitably accompanying the presence of aggregated multi-atomic species. It was suggested in [29] that small carbon clusters play an important role in the generation of high-order harmonics of plasmas. Similar conclusion was made in [30] with regard to TH emission. It was underlined that harmonics generation in plasmas, when performed with full temporal delay control and under conditions of spatial segregation typical of laser ablation plasmas, provides a method to qualitatively assess cluster size distributions for different materials and irradiation conditions.

In graphite the ablation plasma plume may contain various species of carbon, i.e. neutrals and ions, small molecules, clusters, aggregates, etc., which can contribute to harmonic generation to various extent. It is important to determine their presence in the region, where the driving laser pulse interacts with the expanding plasma. In particular, the production of clusters in the laser plasma during laser ablation of various targets has a high probability, while their presence in the plasma area where the frequency conversion occurs was yet to be confirmed directly.

Earlier, the analysis of carbon cluster composition of the ablation plume produced by nanosecond laser pulses for HHG was accomplished by time-of-flight mass spectroscopy (ToFMS) [31], which confirmed the presence of carbon clusters ranging from C_5 to C_{25} . The attempts to find higher mass clusters failed, though they were searched for over a long range of delays up to a few μs between the onset of laser ablation and the switching on the triggering pulse in ToFMS. Earlier studies of carbon plasma have also shown that the $4n + 3$ clusters in $C_5 - C_{25}$ range had higher abundance than neighboring ones [16,32]. The conclusion was made that those clusters (C_7 , C_{11} , C_{15} , and C_{19}) could be considered as the most effective emitters of harmonics.

The harmonic generation in such plasma can prove or disapprove the role of complex composition of ablated species in the former process. A signature revealing the nature of the emitters could be the growth of harmonics emission arising at some specific delay from the beginning of ablation. This delay may characterize the time of propagation of the clusters from the target's surface to the optical axis of ultrashort pulse propagation. It was suggested in [33] that if the components could be assumed to reach thermodynamic equilibrium during the expansion, so that a similar average kinetic energy $E = mv^2/2$ could characterize all plasma components, the average arrival times could be assigned to different cluster sizes. To our opinion this formula rather determines the condition of the similar velocities for the atoms and multiatomic systems

of similar elements, like carbon and fullerene. The similar assumption can be applied to atoms and ions of different materials, which was confirmed during our comparative THG studies using indium and graphite plasmas. The delay at which TH reaches its maximum intensity should scale as a square root of atomic weight, as was demonstrated in present studies [Fig. 3(d)]. The ejection of lighter atoms and ions from the target surface does not allow them reach the axis of the driving beam earlier as compared with heavier species.

Following the logic of Ref. [33], the large clusters like C_n should appear in the laser-plasma interaction zone $n^{0.5}$ times later compared with single atoms and ions of carbon. In other words, the appearance of the group of C_7 – C_{19} clusters in the interaction zone could be expected at delays of 2.7 to 4.4 times later compared to the C_1 particles. However, this scenario does not happen, since no enhancement of harmonics occurred at these delays (90–140 ns). Our studies showed that carbon clusters arrive at the area of interaction with femtosecond beam notably earlier than one can expect assuming the above kinetic equation. In other words, from the very beginning all atoms in clusters acquire a similar kinetic energy and spread out of surface with the velocity approximately equal to the one of a single atom of carbon.

Below, we address the difference in the expected and actual optimal delays between heating and driving pulses in the case of graphite-ablated plasma. In the case of a thermalized ablation plume, i.e. at very slow heating conditions, the average arrival times can be assigned to different cluster sizes. Another situation occurs in the case of the fast, either nanosecond, or picosecond, ejection of energy in the tiny area of the target. In that case the delay between heating and driving pulses at which the harmonic yield reaches its maximum should scale as a square root of the atomic or molecular weight of the constituents. Our additional studies revealed that, for bulk gold ablation, the maximum high-order harmonic yield from single gold atoms and ions occurred at a delay of about 180–300 ns. Meantime, the ablated 20-nm Au nanoparticles allowed efficient generation at about 200–350 ns delay, which is approximately equal to the delay in the case of Au atoms and ions. Furthermore, attempts to observe HHG at the delays of up to 50 μ s, i.e., at the expected delay for thermalized larger nanoparticles, did not show any harmonic emission. Thus, our studies demonstrate that clusters, quantum dots, and relatively small nanoparticles arrive in the area of interaction with the femtosecond laser beam notably earlier than one would expect assuming the thermalized regime of evaporation. In other words, all multi-atomic species acquire, from the very beginning, a similar kinetic energy and spread out from the surface with velocities approximately similar to those of the single atoms and ions ablating from bulk material. This conclusion reconciles the similarity in the optimal delays for HHG from the plasmas produced on the bulk target leading to evaporation of atoms and ions and on the targets containing nanoparticles of the same material.

The velocities of the multi-atomic carbon clusters, which assume to be the main and most efficient emitters of third and higher-order harmonics, are estimated by knowing the “optimal” delays for highest harmonic yields in both cases (~ 100 and ~ 25 ns) and the distances from targets in these two groups of experiments (0.6 and 0.2 mm). These particles possessed the 6×10^3 and 8×10^3 m s⁻¹. One can see a similarity of the velocities determined from the two groups of experiments using different facilities.

More in-depth physical explanation why clusters of various masses seem to spread with a velocity similar to that of a single atom is required in spite of the experimental confirmation of this fact and our assumptions. To resolve this issue, the ToFMS studies can give a convincing answer on the presence of both ion and cluster clouds at the same moment in the area of propagation of the converting pulses. In the meantime, one can assume the difficulties in establishing such sort of experiments requiring the combined HHG and mass spectrometry facilities.

6. Conclusions

In this paper we examined the role of small carbon clusters, which inevitably appear during graphite ablation, in generation of high-order harmonics. The advantage of proposed method for laser ablation and delay-dependent study of harmonic emission during ablation of graphite target is that plasma formation in double-laser configuration of HHG experiments could be efficiently applied for variation of the delay between heating and driving pulses using electronic methods. It can also be applied for other clustered targets to determine the best conditions for HHG in such plasmas. We have demonstrated the advanced properties of the carbon plasma produced by nanosecond pulses as a medium for efficient low- and high-order harmonic generation. The role of $C_5 - C_{25}$ clusters in the enhancement of harmonic generation efficiency has been analyzed. Our HHG studies have demonstrated that these carbon clusters appearing during ablation of graphite influence HHG efficiency at the delays similar to those at which single carbon atoms and ions arrive in the area of femtosecond beam propagation. Our studies have shown that such clusters commonly appearing during time-of-flight mass spectroscopic studies of carbon ablation strongly influence the harmonics yield and thus could be considered as the sources of efficient harmonics in the 40–100 nm spectral range.

Funding

National Key Research and Development Program of China (2017YFB1104700); National Natural Science Foundation of China (NSFC) (61705227, 61774155); Chinese Academy of Sciences (CAS) (2018VSA0001, President's International Fellowship Initiative).

References

1. S. Hädrich, M. Krebs, A. Hoffmann, A. Klenke, J. Rothhardt, J. Limpert, and A. Tünnermann, "Exploring new avenues in high repetition rate table-top coherent extreme ultraviolet sources," *Light: Sci. Appl.* **4**(8), e320 (2015).
2. X. Geng, S. Zhong, G. Chen, W. Ling, X. He, Z. Wei, and D. E. Kim, "Enhancement of high-order harmonics in a plasma waveguide formed in clustered Ar gas," *Opt. Express* **26**(3), 3067–3074 (2018).
3. R. A. Ganeev, V. V. Strelkov, C. Hutchison, A. Zair, D. Kilbane, M. A. Khokhlova, and J. P. Marangos, "Experimental and theoretical studies of two-color pump resonance-induced enhancement of odd and even harmonics from a tin plasma," *Phys. Rev. A* **85**(2), 023832 (2012).
4. A. M. Perego, S. K. Turitsyn, and K. Staliunas, "Gain through losses in nonlinear optics," *Light: Sci. Appl.* **7**(1), 43 (2018).
5. B. D. Bruner, M. Krüger, O. Pedatzur, G. Orenstein, D. Azoury, and N. Dudovich, "Robust enhancement of high harmonic generation via attosecond control of ionization," *Opt. Express* **26**(7), 9310–9322 (2018).
6. R. A. Ganeev, T. Witting, C. Hutchison, F. Frank, M. Tudorovskaya, M. Lein, W. A. Okell, A. Zair, J. P. Marangos, and J. W. G. Tisch, "Isolated sub-fs XUV pulse generation in Mn plasma ablation," *Opt. Express* **20**(23), 25239–25248 (2012).
7. A. Bahabad, O. Cohen, M. M. Murnane, and H. C. Kapteyn, "Quasi-phase-matching and dispersion characterization of harmonic generation in the perturbative regime using counterpropagating beams," *Opt. Express* **16**(20), 15923–15931 (2008).
8. R. A. Ganeev, V. Tosa, K. Kovács, M. Suzuki, S. Yoneya, and H. Kuroda, "Influence of ablated and tunneled electrons on the quasi-phase-matched high-order harmonic generation in laser-produced plasma," *Phys. Rev. A* **91**(4), 043823 (2015).
9. R. A. Ganeev, P. A. Naik, H. Singhal, J. A. Chakera, M. Kumar, M. P. Joshi, A. K. Srivastava, and P. D. Gupta, "High order harmonic generation in carbon nanotube-containing plasma plumes," *Phys. Rev. A* **83**(1), 013820 (2011).
10. C. Vozzi, M. Nisoli, J.-P. Caumes, G. Sansone, S. Stagira, S. De Silvestri, M. Vecchiocattivi, D. Bassi, M. Pascolini, L. Poletto, P. Villoresi, and G. Tondello, "Cluster effects in high-order harmonics generated by ultrashort light pulses," *Appl. Phys. Lett.* **86**(11), 111121 (2005).
11. S. Ghimire, A. D. DiChiara, E. Sistrunk, P. Agostini, L. F. DiMauro, and D. A. Reis, "Observation of high-order harmonic generation in a bulk crystal," *Nat. Phys.* **7**(2), 138–141 (2011).
12. I. J. Kim, G. H. Lee, S. B. Park, Y. S. Lee, T. K. Kim, C. H. Nam, T. Mocek, and K. Jakubczak, "Generation of submicrojoule high harmonics using a long gas jet in a two-color laser field," *Appl. Phys. Lett.* **92**(2), 021125 (2008).
13. I. Lopez-Quintas, M. Oujja, M. Sanz, M. Martin, R. A. Ganeev, and M. Castillejo, "Low-order harmonic generation in nanosecond laser ablation plasmas of carbon containing materials," *Appl. Surf. Sci.* **278**, 33–37 (2013).
14. Y. Akiyama, K. Midorikawa, Y. Matsunawa, Y. Nagata, M. Obara, H. Tashiro, and K. Toyoda, "Generation of high-order harmonic using laser-produced rare-gas-like ions," *Phys. Rev. Lett.* **69**(15), 2176–2179 (1992).

15. X. W. Li, W. F. Wei, J. Wu, S. L. Jia, and A. C. Qiu, "The influence of spot size on the expansion dynamics of nanosecond-laser-produced copper plasmas in atmosphere," *J. Appl. Phys.* **113**(24), 243304 (2013).
16. W. R. Creasy and J. T. Brenna, "Large carbon cluster ion formation by laser ablation of polyimide and graphite," *Chem. Phys.* **126**(2-3), 453–468 (1988).
17. R. A. Ganeev, M. Suzuki, M. Baba, H. Kuroda, and T. Ozaki, "Strong resonance enhancement of a single harmonic generated in extreme ultraviolet range," *Opt. Lett.* **31**(11), 1699–1701 (2006).
18. H. T. Kim, I. J. Kim, D. G. Lee, K.-H. Hong, Y. S. Lee, V. Tosa, and C. H. Nam, "Optimization of high-order harmonic brightness in the space domains," *Phys. Rev. A* **69**(3), 031805 (2004).
19. F. Brandi, F. Giammanco, and W. Ubachs, "Spectral redshift in harmonic generation from plasma dynamics in the laser focus," *Phys. Rev. Lett.* **96**(12), 123904 (2006).
20. R. A. Ganeev, M. Suzuki, P. V. Redkin, M. Baba, and H. Kuroda, "Variable pattern of high harmonic spectra from a laser-produced plasma by using the chirped pulses of narrow-bandwidth radiation," *Phys. Rev. A* **76**(2), 023832 (2007).
21. A. M. Rubenchik, M. D. Feit, M. D. Perry, and J. T. Larsen, "Numerical simulation of ultra-short laser pulse energy deposition and transport for material processing," *Appl. Surf. Sci.* **127-129**(2), 193–198 (1998).
22. H. Ruf, C. Handschin, R. Cireasa, N. Thire, A. Ferre, S. Petit, D. Descamps, E. Mevel, E. Constant, V. Blanchet, B. Fabre, and Y. Mairesse, "Inhomogeneous high harmonic generation in krypton clusters," *Phys. Rev. Lett.* **110**(8), 083902 (2013).
23. V. Veniard, R. Taieb, and A. Maquet, "Atomic clusters submitted to an intense short laser pulse: A density-functional approach," *Phys. Rev. A* **65**(1), 013202 (2001).
24. F. Bourquard, A.-S. Loir, C. Donnet, and F. Garrelie, "In situ diagnostic of the size distribution of nanoparticles generated by ultrashort pulsed laser ablation in vacuum," *Appl. Phys. Lett.* **104**(10), 104101 (2014).
25. T. E. Itina, K. Gouriet, L. V. Zhigilei, S. Noël, J. Hermann, and M. Sentis, "Mechanisms of small clusters production by short and ultra-short laser ablation," *Appl. Surf. Sci.* **253**(19), 7656–7661 (2007).
26. H. O. Jeschke, M. E. Garcia, and K. H. Bennemann, "Theory for the ultrafast ablation of graphite films," *Phys. Rev. Lett.* **87**(1), 015003 (2001).
27. L. B. Elouga Bom, Y. Pertot, V. R. Bhardwaj, and T. Ozaki, "Multi- μ J coherent extreme ultraviolet source generated from carbon using the plasma harmonic method," *Opt. Express* **19**(4), 3677–3685 (2011).
28. M. López-Arias, M. Oujja, M. Sanz, R. de Nalda, R. A. Ganeev, and M. Castillejo, "Generation of low-order harmonics in laser ablation plasmas," *Mol. Phys.* **110**(15-16), 1651–1657 (2012).
29. R. A. Ganeev, "Involvement of small carbon clusters in the enhancement of high-order harmonic generation of ultrashort pulses in the plasmas produced during ablation of carbon-contained nanoparticles," *Opt. Spectrosc.* **123**(3), 351–364 (2017).
30. M. Oujja, J. G. Izquierdo, L. Bañares, R. de Nalda, and M. Castillejo, "Observation of middle-sized metal clusters in femtosecond laser ablation plasmas through nonlinear optics," *Phys. Chem. Chem. Phys.* **20**(25), 16956–16965 (2018).
31. R. A. Ganeev, C. Hutchison, T. Witting, F. Frank, W. A. Okell, A. Zaïr, S. Weber, P. V. Redkin, D. Y. Lei, T. Roschuk, S. A. Maier, I. López-Quintás, M. Martín, M. Castillejo, J. W. G. Tisch, and J. P. Marangos, "High-order harmonic generation in graphite plasma plumes using ultrashort laser pulses: a systematic analysis of harmonic radiation and plasma conditions," *J. Phys. B* **45**(16), 165402 (2012).
32. A. Kaplan, M. Lenner, C. Huchon, and R. E. Palmer, "Nonlinearity and time-resolved studies of ion emission in ultrafast laser ablation of graphite," *Appl. Phys. A* **92**(4), 999–1004 (2008).
33. R. de Nalda, M. Lopez-Arias, M. Sanz, M. Oujja, and M. Castillejo, "Harmonic generation in ablation plasmas of wide bandgap semiconductors," *Phys. Chem. Chem. Phys.* **13**(22), 10755–10761 (2011).